Influence of nanosized confinements on 4-*n*-decyl-4′-cyanobiphenyl (10CB): A broadband dielectric study

J. Leys, G. Sinha,* C. Glorieux, and J. Thoen
Laboratorium voor Akoestiek en Thermische Fysica, Departement Natuurkunde en Sterrenkunde, Katholieke Universiteit Leuven, Celestijnenlaan 200D, B-3001 Leuven, Belgium
(Received 11 October 2004; published 11 May 2005)

Real (ϵ') and imaginary (ϵ'') parts of the complex dielectric permittivity (ϵ^*) of the liquid crystal (LC) 4-*n*-decyl-4′-cyanobiphenyl (10CB) embedded in Anopore membranes and Vycor porous glass, as well as dispersed with hydrophilic aerosils, have been studied by means of broadband dielectric spectroscopy in the frequency range from 10^{-2} Hz to 1 GHz. In bulk 10CB, which has a direct transition from an isotropic to a smectic-*A* phase, there exists one main relaxation process for the parallel orientation of the director with respect to the probing field and a faster one for the perpendicular orientation. All molecular relaxation processes in 10CB are of Debye type and have Arrhenius like temperature dependence. For 10CB embedded in untreated and surface treated cylindrical pores of Anopore membranes the dielectric spectra are similar to the bulk with the exception that both the rotation around the short axis and the libration motion are faster in the pores. In the case of 10CB dispersed with two different concentrations of hydrophilic aerosils an emergence of a slow relaxation process, which is stronger for the higher concentration, is additionally observed along with the bulklike processes. The slow process in the LC-hydrophilic aerosil system is attributed to the relaxation of the molecules that are homeotropically aligned close to the surfaces of the aerosil particles. This process also has an Arrhenius type of temperature dependence. For 10CB embedded in narrow channels of Vycor porous glass three relaxation processes are observed. Two of these processes are bulklike and are due to the librational motion of molecules and the rotation of molecules around their short axes. The slowest process seems to be a surface process, similar in origin to that observed for 10CB dispersed with hydrophilic aerosils, and is prominent amongst all. The material in the Vycor porous glass could be supercooled by at least 185° below bulk crystallization temperature. The slow process has a Vogel-Fulcher-Tamman (VFT) type of temperature dependence typical for glass formers in this wide temperature range. In addition, the bulklike processes are found to be strongly modified and also have a VFT like temperature dependence from measurements done in a wide temperature range. This behavior is in contrast to other reports of glassy behavior in confined LC, where the glassy behavior as concluded from a slow relaxation process observed in a narrow temperature range.

DOI: 10.1103/PhysRevE.71.051709 PACS number(s): 61.30.−v, 68.08.−p, 77.22.Gm

I. INTRODUCTION

Confining and dispersing soft condensed matter has been a field of active research for more than a decade, which has captivated the minds of several scientists either looking for fundamental changes in the physical properties of the material or searching for new applications [1–6]. In most of these studies the influence of the large interfacial area and the diminutive size of the confining channels, which are inherent characteristics of these systems, have been exploited. They have usually focused on the issue of structure, phase and glass transitions, as well as dynamics of molecular motion in these systems [7–20]. Several theoretical and experimental review articles have also been devoted to this subject [21–24]. New and interesting results in this interesting area come up from time to time. One such work is a study of ethylene glycol (EG) confined to zeolitic host systems of different topology [25]. The experiment deals with the transition of the dynamics of isolated molecules to that of a bulk liquid. It was found in this study that below a threshold pore size the liquid character of EG disappeared, which was indicated by a dramatic increase in the relaxation rate and an Arrhenius-like temperature dependence of this glass former. In another important study, evidence of a glassy behavior for LC in sintered porous silica (SPS) glass was first presented in 1992 by Wu *et al.* in a quasielastic light scattering experiment [8]. The change in the dynamical behavior of confined LC was explained by considering a weak random anisotropy imposed by the silica gel on the liquid crystalline phase. A similar experiment of LC in a aerogel host, where the ordered domains in the nematic phase are comparable to the pore size, comparable slow glasslike relaxation was also observed [26]. In both cases of SPS and aerogel hosts the correlation functions showed divergent slow decays, diverging from above at a temperature around $T^* = 32.2\,^\circ\mathrm{C}$, from which the orientational glassy behavior were concluded. In another study of nematic LC dispersed with hydrophilic aerosils by a turbidity experiment and simulations, remnant order and slow dynamics indicative of an induced nematic glass state was also observed [27]. Some theoretical work supporting glassy state in nematics with quenched disorder have also been reported where a short-ranged ordered phase was found along with a quasi-long-range ordered phase [28]. In a photon correlation spectroscopic and dielectric study of

*Author to whom correspondence should be addressed. Email address: GhanshyamPrasad.Sinha@fys.kuleuven.ac.be

 ©2005 The American Physical Society

5CB confined in porous matrices with randomly oriented and interconnected pores with size around 100 Å deep supercooling and glassy behavior was also briefly reported [29]. Evidence of a glassy behavior was also present in the deuteron NMR measurements, with a high temperature and spectral resolution, of 8CB confined to the randomly interconnected pores of silica aerogel [30]. In most of the above mentioned important works, glassy behavior were concluded from slow dynamics with features of a non-Arrhenius behavior of the relaxation process in a limited temperature range of liquid crystalline phases. In this paper we show results where the glassy behavior could be obtained due to deep supercooling that eventually led to a non-Arrhenis dependence of the relaxation times of bulklike processes as well as a slow relaxation process.

Confined systems have a high surface-to-volume ratio that can be exploited in experiments that are sensitive to physical behavior near the surfaces. Dielectric spectroscopy is one such method that can be used to characterize the influence of confinement on the dynamical aspects of soft condensed matter. An additional advantage of this method is the wide range of accessible frequencies that can be employed successfully in cases where a glassy behavior is investigated. The slowing down of the relaxation process due to glass formation can lead to dramatic changes in the observed characteristic frequency especially if the sample is measured over a wide temperature range. The method is also suitable for lineation with high accuracy the relaxation times as a function of temperature [31]. Application of dielectric spectroscopy to liquids and liquid crystals in the past has revealed new information on the changes in the molecular mobility, the broadening of the distribution of relaxation times, as well as changes in the phase and the glass transition temperatures [10,11,15–18,25]. New relaxational modes have been observed in several studies of confined LCs, which have been attributed to the relaxation of molecules in the vicinity of the pore surface [3,11,15,16,32,33]. In the dielectric study of alkylcyanobiphenyls dispersed in porous matrices with randomly oriented, interconnected pores with two different pore sizes, a slow relaxation process around 100 kHz was observed, which was attributed to the presence of a surface layer at the solid pore wall–LC interface [32]. In another dielectric relaxation and polarization decay experiments of pure 5CB and 5CB in trinuclear pyrimidine glasslike behavior was deduced from measurements done at fast cooling rates [34]. The relaxation times obtained by dielectric spectroscopy of the bulklike processes of 5CB, which has only a nematic phase, in Geltech porous glass also show a Vogel-Fulcher-Tamman (VFT) type of temperature dependence [35]. However, this unusual behavior of confined 5CB has not been discussed in the paper.

Recently, applying internal restrictions on liquid crystals by introducing nanosized silica particles into the phase have also started to be investigated in great detail [9–11,15–17]. In the dielectric study of a quasi-two-dimensional system of 4-*n*-alkyl-4′-cyanobiphenyl (*n*CB) LC dispersed with aerosil nanoparticles, a slow relaxation was detected at temperatures below the bulk crystallization temperature, which was attributed to the relaxation of molecules in the surface layers [10,11]. The temperature dependence of the relaxation times for the slow process showed behavior typical for glass-forming liquids. For similar other studies of alkylcyanobiphenyls dispersed with hydrophilic and hydrophobic aerosils, the presence of a slow relaxation process in the case of hydrophilic aerosils were attributed to the relaxation of molecules in surface layers [15,16]. The slow relaxation process is due to the rotation of molecules around their short axis for molecules that are close to the surface of the aerosils. This process is slower than the bulk rotation around the short axis because the viscosity in the surface layers are greater than the bulk viscosity. The cause of the higher viscosity could be due to the preference of the dipole moments that are at the edge of the *n*CB molecules to hydrogen bond with the silanol groups present at the surface of the aerosils [16].

Most of the studies, in general, have focused on the influence of confinement on the continuous nematic to smectic phase transition. More recently, examining the effect of dispersed aerosils in LCs that have a direct transition from an isotropic phase to a smectic-*A* phase (with one-dimensional translation order), without any nematic phase, have been reported by two groups [20,36]. In such materials differences from systems with an intervening nematic phase have been observed. In both studies it was observed that part of the direct isotropic-smectic first order character was retained. However, in one of them the correlation lengths were observed to increase discontinuously and saturate at the phase transition [36] while in the other the smectic correlation length decreased more slowly with increasing aerosils concentrations. Furthermore, in another recent study on a LC with direct isotropic–smectic-*A* (*I*-Sm*A*) transition embedded in surfactant treated Anopores, a surface-induced orientational ordering above the smectic-isotropic transition was found to exist [14]. Surface-induced layering and molecular self-diffusion models were used to explain this effect. Such effects were, however, not observed for LCs that have an intervening nematic phase. Studies on similar liquid crystals bounded by silane treated solid substrate using evanescent-wave ellipsometry revealed interesting results where an interfacial region was found in 10CB, above the *I*-Sm*A* transition, which was suggested to be in a nonspontaneous nematic phase induced by the surface-LC interaction field. This interfacial region was calculated to have a thickness around one molecular length [37]. The other liquid crystals 11CB and 12CB did not show any surface ordering behavior whatsoever.

In the light of the fact that differences in the behavior were observed between LCs that have an intervening nematic phase and the ones without, we have performed dielectric measurements on 4-*n*-decyl-4′-cyanobiphenyl (10CB), with several different types of confinement. We used Anopore membranes as cylindrical confinements that comes in only one pore size. We also dispersed 10CB with different concentrations of hydrophilic aerosils. The aerosil particles can form a hydrogen bonded three dimensional network above a gelation threshold $\rho_s \sim 0.01\ \mathrm{g/cm^3}$ where, ρ_s is the weight of silica per $\mathrm{cm^3}$ of LC [38]. For very small confinements, we used Vycor porous glass, which also comes in a single pore size. Our motive was to use different types of confinement and see the influence of diverse confining materials on one liquid crystal that has a direct transition from

an isotropic phase to a smectic phase. The paper is organized as follows. In Sec. II we describe our samples and the experimental setup. The information on phase transition temperatures of 10CB is also given in the section along with the information about the confinements. In Sec. III we present the static values of the dielectric permittivity of bulk and confined 10CB. Here we show a different temperature dependence of the static dielectric permittivity in comparison to the lower homologues of 10CB and a plausible explanation. In Sec. IV we show representative dielectric spectra of 10CB observed at various temperatures under different confinements where we also show the observation of a slow relaxation process in two samples: 10CB with hydrophilic aerosils and 10CB embedded in Vycor porous glass. We also describe the characteristic features of all spectra observed in this section. Section V is devoted to a discussion of the temperature dependence of relaxation times of bulk-like processes as well the surface process. We also show here that all the processes show activated type of dynamics in Anopore and aerosils host systems, whereas features of glass formation become evident from a wide temperature range covering at least 200°.

II. EXPERIMENT

We have measured 4-*n*-decyl-4′-cyanobiphenyl (10CB), under different confinements, namely, the cylindrical pores of Anopore membranes, two high concentrations of hydrophilic aerosils and porous Vycor glass of type 7930. 10CB was obtained from BDH Chemicals Ltd. and was used without further purification. The material has a direct isotropic to Sm*A* transition at 50.2 °C. It generally crystallizes at 44.0 °C. The three different types of confinement had confining sizes varying from 2000 Å to 40 Å.

We studied 10CB confined in untreated and lecithin treated cylindrical pores of Anopore membranes with nominal pore sizes of 2000 Å obtained from Whatman. The LC-Anopore membrane samples were prepared in the following way. First of all, the membranes were dried overnight at 200 °C in a jar kept under vacuum. For the preparation of the untreated samples, the dried membranes were impregnated with the LC, inside a nitrogen chamber, at a temperature well above the smectic *A* to isotropic (Sm*A*-*I*) transition temperature $T_{AI} \sim 50.2$ °C (the LC thus remaining in the isotropic phase). However, in the case of treated membranes, in order to obtain a homeotropic orientation at the pore wall, the matrix was dipped in a 3% weight solution of lecithin in hexane, for 1 h. The treated membrane was then kept overnight under vacuum to ensure the complete evaporation of hexane before impregnating it with the LC. During this preparation step 10CB was kept in the isotropic phase. In both cases of treated and untreated samples the excess LC on the top surface of the membrane was carefully wiped with tissue papers, at a temperature above T_{AI}.

For intermediate sizes of confinement we studied 10CB dispersed with hydrophilic aerosils. Two different concentrations of hydrophilic aerosils were prepared with ρ_s equal to 0.08 and 0.31 g cm^{-3}, where

$$\rho_s = \frac{m_s}{m_{LC}}\rho_{LC} \approx \frac{m_s}{m_{LC}}(1\ \mathrm{g\ cm^{-3}}). \tag{1}$$

m_s and m_{LC} are the masses of the aerosils and LCs used in the mixture preparation. For this preparation, hydrophilic aerosils of type 300 were obtained from Degussa Corp. The hydrophilic aerosils of type 300 had diameters around 70 Å and surface area 300 ± 30 m^2/g. On the surface of hydrophilic aerosil, there is one silanol group (≡Si—OH) per 0.28–0.33 nm^2. Hence the aerosils we used have about 9.7×10^{20} silanol groups per gram [39]. If we use the method of calculating the size of the confinement from Ref. [40] then the size of the domains of LCs can be obtained from the relation $\ell_0 = 2/a\rho_s$, where ℓ_0 is the length scale, a is the surface area of the aerosils (~ 300 m^2 g^{-1}), and ρ_s is $(m_s/m_{LC})\rho_{LC}$. On using such a relation we obtain the aerosil void sizes where the LC molecules reside as 833 Å for 0.08 and 215 Å for 0.31 g cm^{-3} of hydrophilic aerosils, respectively. The sample preparation method has been described in Ref. [16].

Measurements were also performed on a system with very small pore sizes comparable to the molecular size. We embedded 10CB inside porous Vycor glass 7930 obtained from Corning Inc. Vycor porous glass has a network of three-dimensional randomly connected pore segments with a mean pore diameter ~70 Å, having a distribution width of ~5 Å, and an average chord length ~300 Å [41]. Detailed properties of Vycor glass have been reported earlier in Ref. [42]. The porous glasses were first cleaned with concentrated nitric acid at 100 °C and then washed with deionized water several times. The glass was then baked overnight at 450 °C. The glass was finally impregnated with the LC at a temperature above T_{AI}.

Measurements of the real (ϵ') and the imaginary (ϵ'') parts of the complex dielectric permittivity were done with different combinations of impedance analyzers and LCR meters. For the bulk as well as 10CB in Anopores and Vycor porous glass, the measurements were performed using NOVOCONTROL broadband dielectric spectrometer in the frequency range from 10^{-2} Hz to 1 MHz, which consists of a high resolution dielectric/impedance analyzer ALPHA and an active sample cell. In the frequency range from 1 MHz to 1 GHz the HP4291B RF impedance analyzer was used in combination with a home made cell [15]. For bulk measurements both sides of the electrodes were, beforehand, spin coated with polyimides to obtain the necessary alignment. We used the polyimide SE1211 (Nissan Chemicals) for the parallel measurements (director parallel to probing electric field). We verified that optical cells made from SE1211 coated glass slides resulted in homeotropic alignment for 10CB before coating on the polished metal electrodes used in the dielectric permittivity measurements. For perpendicular measurements (director perpendicular to probing electric field) PI2555 (HD Microsystems) was similarly coated on the electrodes and rubbed uniaxially to obtain the required planar alignment. A test with an optical cell under the microscope was also done beforehand to verify the achievement of the required alignment. In the two cases of polyimide coatings, the sample was placed between two polished electrodes

separated by two optic fiber spacers 50 μm in diameter. For the Anopore and Vycor samples the measurements were done without any surface treatment of the electrodes. For the temperature control in the low frequency measurements the NOVOCONTROL four circuit Quatro system was used. The temperature control in the high frequency measurements were similar to that described in Ref. [43]. For the LC dispersed with aerosils a polyimide coated surface was not convenient, hence the measurements were done in the frequency range from 75 kHz to 30 MHz using a Hewlett-Packard HP4285A precision LCR meter where we had an option of applying a high electric field to orient the director parallel to the probing field. The details of the measurement procedure are described in Ref. [44]. The sample cell consisted of a parallel plate capacitor type with a guard ring that eliminated the stray capacitance caused by the edge effect. The distance between two electrodes was about 200 m. The temperatures were controlled using an oven designed to accommodate the low frequency cell [15].

The software package WINFIT provided by NOVOCONTROL was used for the data analysis. For the quantitative analysis of the dielectric spectra we used the Havriliak-Negami function [45] which is incorporated in the WinFIT software. For the case of more than one relaxation process, taking into account the contribution of the dc conductivity to the imaginary part of dielectric permittivity, the Havriliak-Negami function in the frequency domain is given as

$$\epsilon^* = \epsilon_\infty + \sum_j \frac{\Delta\epsilon_j}{[1+(i2\pi f\tau_j)^{1-\alpha_j}]^{\beta_j}} - i\frac{\sigma}{2\pi\epsilon_0 f^n}, \qquad (2)$$

where ϵ_∞ is the high-frequency limit of the permittivity, $\Delta\epsilon_j$ the dielectric strength, τ_j the mean relaxation time, and j the number of the relaxation process. The exponents α_j and β_j describe the symmetric and asymmetric distribution of relaxation times. The term $i\sigma/2\pi\epsilon_0 f^n$ accounts for the contribution of conductivity σ, with n as fitting parameter.

III. STATIC DIELECTRIC PERMITTIVITY OF BULK AND CONFINED 10CB

The temperature dependence of the static dielectric permittivity ϵ' of bulk 10CB and 10CB under different confinements, for $\mathbf{E}\|\mathbf{n}$ and $\mathbf{E}\perp\mathbf{n}$ orientations, is shown in Fig. 1. The quantities $\epsilon_\|$ and $\epsilon_\perp$ represent the dielectric permittivity values measured at 115 kHz for the probing electric field $\mathbf{E}$ parallel and perpendicular to the macroscopic molecular orientation $\mathbf{n}$, respectively. Just for a test the static values were measured in the isotropic phase without any polyimide coating to see the influence the thin polymer layer on the capacitance of the sample. The values in such case were about 2% higher than with a coating. Hence the influence of the polyimide coating on the measured values of the dielectric permittivity was within the experimental error. The dielectric anisotropy $\Delta\epsilon(=\epsilon_\|-\epsilon_\perp)$ in the smectic phase was found to decrease with decreasing temperature. This behavior is similar to that observed in the smectic phase of 8CB as presented in Ref. [46]. Such a dependence of the dielectric permittivity

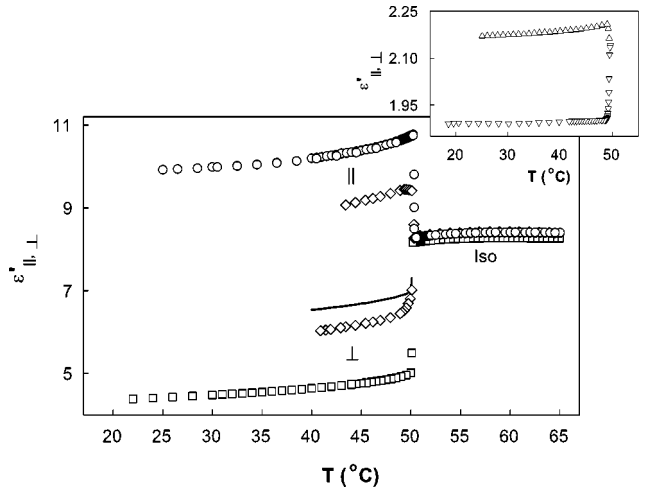

FIG. 1. The temperature dependence of the static dielectric permittivity ϵ' of bulk and confined 10CB: bulk 10CB in the smectic phase with parallel ($\|$, ○) and perpendicular ($\perp$, □) orientations and in the isotropic phase (○); 10CB dispersed with 0.08 g cm^{-3} of aerosils (◇). Solid line represents $(\epsilon'_\| + 2\epsilon'')/3$ of bulk 10CB. Inset: The temperature dependence of the static dielectric permittivity of 10CB impregnated in untreated (△) and treated (▽) matrices of Anopore membranes in the smectic phase.

with respect to temperature could be due to the increase in the anticorrelation factor as we lower the temperature. A similar effect of the anticorrelation factor on $\epsilon_\|$ in the smectic phase was also observed in 4,4′-diheptylazoxybenzene (D7AOB) that has a weak dipole moment compared to *n*CBs [43,47]. In addition the average value $[(\epsilon_\|+2\epsilon_\perp)/3]$ has a large dip after the transition from the isotropic to smectic phase, which is most likely a real effect. This would seem normal if we compare the average value of the static dielectric permittivity of 8CB at the nematic-isotropic (*N*-*I*) transition and *N*-Sm*A* transition. This is probably not due to poor alignment as the alignment was checked under a polarizing microscope by using the same polyimide solution in a glass cell. The cell was made out of two coated glass plates with the same spacers used in the measurement and filled with 10CB under similar conditions. The change from the isotropic value to the smectic value in 8CB would be comparable to 10CB if we imagine there was no nematic phase in 8CB (see Ref. [46]). It is known from the precise measurements of the static values of dielectric permittivity at the *I*-*N* transition a small dip is always observed due to the change in density as obtained from the Clausius-Claperon equation. The density changes occurring at *I*-Sm*A* transitions for 10CB are much greater than those occurring in *I*-*N* transitions [48]. The density changes by 1% in 10CB at the *I*-Sm*A* as compared to 0.2% for 8CB at the *I*-*N* transition. However, the density changes may not be very important in this case as the changes in the Kirkwood correlation factor g could have a greater effect on the static value of the dielectric permittivity. The effective dipole moment, which the dielectric permittivity value depends strongly on, is given by the following expression: $\mu_{eff}^2 = g\mu^2$. The typical changes in the values of g from the isotropic to the smectic phase are much greater than that from an isotropic to a nematic phase [46]. 10CB in the

liquid crystalline phase is probably in a deep smectic phase and hence there could be greater changes in the Kirkwood correlation factor leading to a considerable dip in the static permittivity of 10CB in parallel orientation. The bulk spectra shown later also support the fact that the LC domains are properly aligned and peaks that may occur due to poor alignment are minimal.

The temperature dependence of the static dielectric permittivity ϵ' of 10CB embedded in untreated and in lecithin treated 2000 Å cylindrical pores of Anopore membranes, measured at 1 MHz is shown in Fig. 1 (see inset). The dependence is quite weak for 10CB in Anopore membranes, but quite similar to the temperature dependence of bulk 10CB. Since from different measurements of the dielectric permittivity of Anopore-LC composites, treated and untreated, differences in the absolute values were observed, the values for the treated matrix were adjusted to that of the untreated sample by a multiplicative factor of 0.39. There was also a difference in the transition temperature, which was higher in the treated sample compared to the bulk and lower in the untreated sample. The temperatures of the treated sample were also adjusted to the transition temperature of untreated matrix in the presented graph by shifting it to lower temperatures by 1.75 °C. The small values of the static dielectric permittivity compared to bulk is due to the small amount of LC material present in the pores of the Anopore membranes. The dielectric permittivity of the Anopore membrane, which is made of alumina, is constant and is around 2.1 in the measured temperature range. Thus, the variation in the values of the dielectric permittivity of the composite is mainly due to the changes in the values of the liquid crystalline material.

An example of the static values of dielectric permittivity obtained for 10CB dispersed with aerosils have been included in Fig. 1. The absolute values have been adjusted to the bulk values in the isotropic phase by using a multiplicative factor of 0.95. Shifts in the transition temperatures were also observed. The measured temperatures of the dispersed samples were thus shifted by matching the transition temperatures with respect to the bulk value by subtracting 0.6 °C from the original value. The dependence of the static dielectric permittivity obtained for 10CB with 0.08 g cm^{-3} aerosils is found to be similar to the bulk behavior in the isotropic as well as the liquid crystalline phase. In the smectic phase, the values are less than the bulk values for the parallel orientation and larger than bulk for the perpendicular orientation. These differences are due to the disorder imposed by the aerosil network on the liquid crystalline domains. The effect of the aerosil network was strong enough to induce disorder in the liquid crystalline phase and thus preventing a complete alignment of the director in the direction of the orienting field. The values representing 10CB under perpendicular orientation for the aerosil dispersed sample were, however, obtained without alignment under any electric field and were obtained in the same measurement run as for parallel orientation, but in the cooling run. It seems that the surface interaction between the electrodes (in this case made of stainless steel) and the LC molecules caused perpendicular alignment to the probing field and hence the interaction led to the propagation of such alignment into the phase.

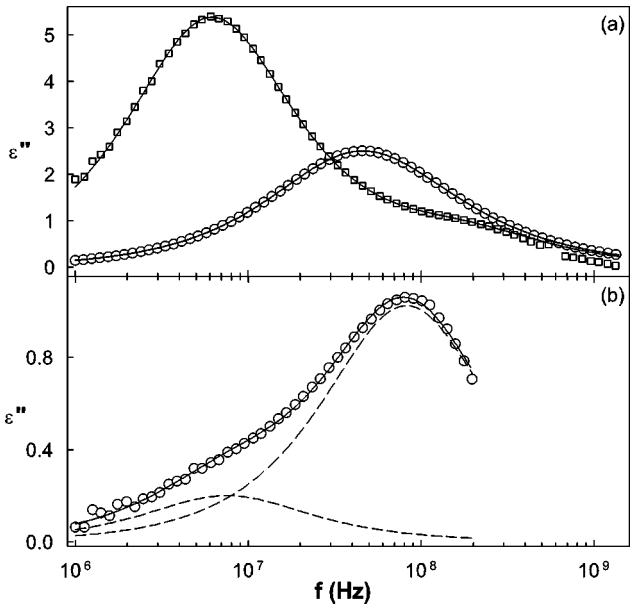

FIG. 2. The imaginary parts of the dielectric permittivity of bulk 10CB in (a) the smectic phase at $T=46$ °C for $\mathbf{E}\|\mathbf{n}$ (□) and the isotropic phase at $T=62$ °C (○); and in (b) the smectic phase at $T=46$ °C for $\mathbf{E}\perp\mathbf{n}$ (○). Solid lines show fitting according to Eq. (2) and the dashed lines represent deconvolution into elementary processes.

IV. DIELECTRIC SPECTRA OF BULK AND CONFINED 10CB

The dielectric spectra of bulk 10CB are similar to the spectra observed for the other series of the cyanobiphenyl group. Typical dielectric spectra obtained for bulk 10CB in the smectic phase (parallel and perpendicular orientations of the director) and in the isotropic phase have been shown in Fig. 2. In the isotropic phase there exists one single relaxation process with characteristic frequencies around 50 MHz. The process is asymmetric as can be seen from Fig. 2(a). The asymmetry was found to reduce with increasing temperature, tending towards a symmetric but broader process compared to that observed at temperatures close to the isotropic-Sm*A* transition. In the smectic phase, for the parallel orientation of the director with respect to the probing field, there exist two adjacent processes with the slower one being clear and prominent and the faster process being of shoulderlike shape. The slower process is due to the rotation of the molecules around their short axes and is of Debye type. The shoulderlike process could be due to the rotation in a cone around the director which is in general faster than the rotation of molecules around short axis [43]. The dielectric strength of the main process has similar temperature dependence, in both smectic and isotropic phase, as observed for the static dielectric permittivity. The behavior of the fast process, however, does not change much with temperature.

In the case of the perpendicular orientation of the director with respect to the probing field we also observe two separate processes [see Fig. 2(b)]. The fast process is more prominent and is assigned as the librational motion of molecules [49]. Since the 10CB molecules do not have a perpen-

TABLE I. Fitting parameters of relaxational processes for bulk and confined 10CB.

T (°C)	$\Delta\epsilon_a$	τ_a (s)	α_a	β_a	$\Delta\epsilon_b$	τ_b (s)	α_b	β_b	$\Delta\epsilon_c$	τ_c (s)	α_c	β_c
bulk 10CB for $\mathbf{E}\parallel\mathbf{n}$												
46.0					10.72	2.66×10^{-8}	0.01	1	1.34	8.80×10^{-10}	0.04	1
62.0					5.65	3.71×10^{-9}	0.05	0.91				
bulk 10CB for $\mathbf{E}\perp\mathbf{n}$												
46.0					0.40	2.11×10^{-8}	0	1	2.06	1.93×10^{-9}	0.01	1
10CB embedded in 2000 Å cylindrical pores												
46.0					0.78	1.91×10^{-8}	0	0.86	0.07	6.93×10^{-10}	0.15	1
62.0					0.65	3.49×10^{-9}	0.02	0.59				
10CB embedded in lecithin treated 2000 Å cylindrical pores												
46.0					0.47	1.49×10^{-9}	0.32	1				
62.0					0.88	3.05×10^{-9}	0.04	0.82				
10CB filled with hydrophilic aerosils at $\rho_s=0.08$ g cm^{-3}												
48.0	0.43	8.96×10^{-7}	0.01	1	6.35	2.20×10^{-8}	0.02	1				
10CB filled with hydrophilic aerosils at $\rho_s=0.31$ g cm^{-3}												
48.0	0.41	6.12×10^{-7}	0.24	1	0.81	2.13×10^{-8}	0	1				
10CB embedded in Vycor porous glass												
60.0	1.97	3.42×10^{-7}	0.35	1	0.57	5.24×10^{-9}	0.13	1	0.73	7.84×10^{-10}	0.28	1
46.0	2.37	2.66×10^{-6}	0.31	0.7	0.48	1.01×10^{-8}	0.11	1	0.47	6.38×10^{-10}	0.27	1
20.5	2.92	5.26×10^{-5}	0.37	0.72	0.65	6.97×10^{-8}	0.33	1	0.45	5.59×10^{-10}	0.33	1
−10.0	3.56	5.04×10^{-2}	0.47	0.41	0.28	1.04×10^{-6}	0.12	1	0.52	7.25×10^{-10}	0.42	1
−50.0	0.78	3.06×10^{-1}	0.30	0.27	0.14	4.86×10^{-3}	0.48	1	0.20	4.71×10^{-8}	0.53	1
−145.0									0.43	1.12×10^{-1}	0.64	0.23

dicular component of the dipole moment, the rotation around the long axis is inactive in the dielectric measurements for such molecules. The slower process could be due to the rotation of molecules around the short axis for those molecules that could not be aligned perfectly parallel to the surface of the coated electrodes. This is quite likely for molecules that are close to the surface as there is always a pretilt of the molecules near the electrodes [43]. The fitting parameters obtained for the curves in Fig. 2 are given in Table I.

In Fig. 3 we present typical spectra obtained for 10CB embedded in 2000 Å cylindrical pores of Anopore membranes, without any surface treatment. In the isotropic phase the relaxation process with characteristic frequency around 50 MHz, comparable to the bulk process, still exists and is asymmetric. The asymmetry reduces with increasing temperature where β is around 0.5 close to the I-SmA transition and 0.6 at $T=65$ °C. In the smectic phase there exists two processes similar to the case of the bulk phase for parallel alignment. However, the fast process is less apparent as compared to the bulk fast process. From the similarity to the bulk spectra for parallel alignment, the dielectric process in untreated Anopore membranes is basically due to the axial alignment of molecules, i.e., the director is oriented along the cylindrical axis of the pores [see Fig. 3(a)]. In the smectic phase the smectic layers are thus oriented perpendicular to the pore axis. In the case of the main process, which is due to the rotation around the short axis, the α parameter is close to 0 at all temperature. The β parameter, however, is close to

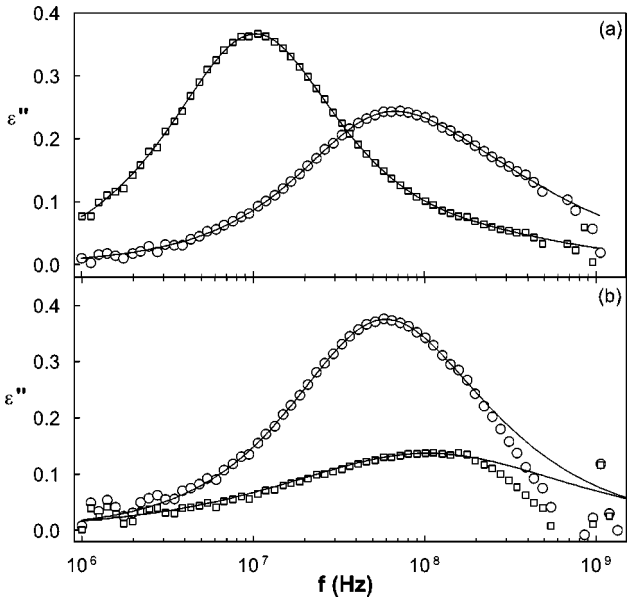

FIG. 3. (a) The imaginary parts of the dielectric permittivity in the smectic phase at $T=46$ °C (□) and isotropic phase at $T=62$ °C (○) of 10CB embedded in untreated 2000 Å cylindrical pores of Anopore membranes. (b) The imaginary parts of the dielectric permittivity in the smectic phase at $T=46$ °C (□) and the isotropic phase at $T=62$ °C (○) of 10CB embedded in lecithin treated 2000 Å cylindrical pores of Anopore membranes. Solid lines show fitting according to Eq. (2).

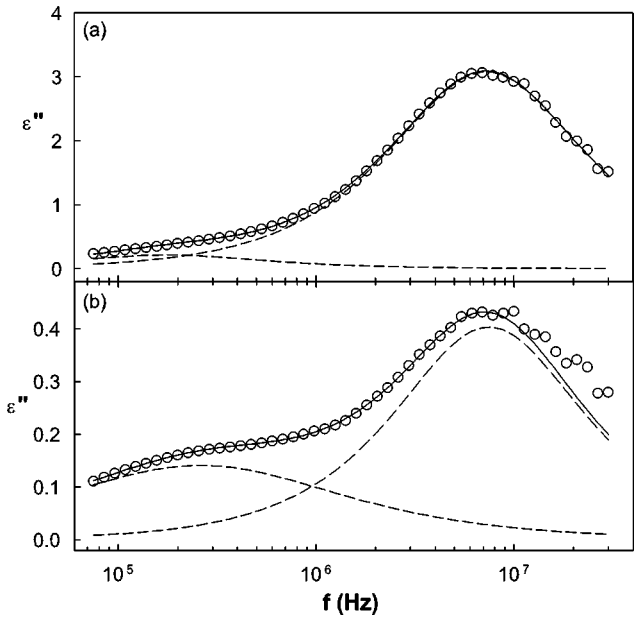

FIG. 4. The imaginary parts of the dielectric permittivity in the smectic phase at $T=48$ °C ($\mathbf{E}\|\mathbf{n}$, ○) of 10CB dispersed with (a) 0.08 g cm^{-3} and (b) 0.31 g cm^{-3} of hydrophilic aerosils. Solid lines show fitting according to Eq. (2). Dashed lines show deconvolution into elementary processes.

0.9 at temperatures corresponding to the smectic phase. The dielectric strength has a similar temperature dependence as for the bulk static value.

In the case of Lecithin treated Anopores the behavior in the isotropic phase, as expected, is similar to that of untreated Anopores. In the smectic phase the process is faster than in the isotropic phase for similar temperatures. The characteristic relaxation frequency is comparable to the main bulk process observed for the perpendicular orientation of the director with respect to the probing field. Thus we can conclude that in the lecithin treated Anopore membranes the orientation of the LC molecules could have a radial orientation in the smectic phase. In the case where the LC director is oriented perpendicular to the probing field we measure the librational mode of the molecules, in the case in which the dipole is along the molecular axis. In our measurements, the cylindrical axis of the pores are parallel to the probing field. Hence in the case of the lecithin treated Anopore membranes, where we have a radial alignment of molecules in the smectic phase, we mainly probe the librational mode of molecules. The fitting parameter α of this process was found to be close to 0 in the isotropic phase which reduces to 0.7 in the smectic phase. The β parameter is close to 0.95 implying a nearly symmetric process. However in the isotropic phase of 10CB in lecithin treated Anopores this parameter is around 0.75 close to the transition temperature that increases to 0.85 at highest measured temperature. The fitting parameters obtained for the curves in Fig. 3 are given in Table I. In summary, the behavior of 10CB molecules in Anopore membranes is similar to the those of the lower homologue series that have a nematic phase.

In Fig. 4 we present typical data for 10CB dispersed with hydrophilic aerosils. The spectra have been presented in the frequency range from 75 kHz to 30 MHz In this frequency range the composite has two clear relaxations. The fast process with characteristic frequencies around 5 MHz is of molecular origin and is due to rotation of molecules around short axis. The slower process has characteristic frequencies comparable to those observed for 7CB and CB15 dispersed with hydrophilic aerosils [15,16]. The origin of the slow process, similarly, could also be due to the hindered rotation of molecules in the vicinity of the surface area of aerosils. The process depends on the density of the aerosil particles as is evident by comparing Figs. 4(a) and 4(b). By increasing the concentration of the particles we basically increase the surface area of interaction of the LC molecules with the aerosil particles, which have several-OH groups on its surface. In the sample with higher concentration of aerosils we could not achieve a parallel orientation of the director, as the applied strong electric field was not effective enough. This has also led to the scatter in the data at high frequencies as seen in Fig. 4(b). The characteristics of the slow relaxation process were found to be similar in character in all phases, namely nematic, smectic and isotropic phases. The process, however, was quite wide that means the relaxation process has a broad distribution of relaxation times. The fitting parameter α obtained in 10CB with aerosils was around 0.3 for all temperatures and the process was found to depend weakly upon temperature. The fitting parameters obtained for the curves in Fig. 4 are given in Table I. This sample also showed features that were similar to the lower homologues of 10CB dispersed with hydrophilic aerosils.

The dielectric spectra of 10CB embedded in porous Vycor glass was found to be completely different from those samples presented before (compare Fig. 5 with previous relaxation spectra). However, on closer scrutiny some relation with the previously observed relaxation processes in 10CB under confinement could be established. First of all, we can see that at least three clear relaxation processes are visible from the dielectric spectra. On comparing the characteristic frequencies the fastest process can be related to the bulklike libration motion, for molecules that are perpendicular to the probing field. In Vycor the pores are randomly oriented in space and so there are molecules oriented parallel as well as perpendicular to the probing electric field at the same time. The second intermediate process could also be a bulklike process that is due to the rotation of molecules around short axis. Both these bulklike processes are weak in strength in comparison to the slowest relaxation process. Since the pore size of Vycor is around 40 Å that is around twice the molecular length of 10CB molecules, most of the molecules are in the vicinity of the surface, and only a few molecules are "free" as it would had been in bulk. This is reflected in a weak dielectric strength of the bulklike processes and a stronger slower process we, hereafter, refer to as the surface process. Vycor glass contains 96% silica and hence would have similar surface characteristics as aerosils made from fumed silica and there are several-OH groups on the surfaces of the pores [50]. Hydrogen bonding between the these hydroxyl groups and the polar part of the LC molecules can lead to a considerable slowing down of the rotational process. Similar type of hydrogen bonding were also reported for strongly interacting polar liquids, such as pyridine,

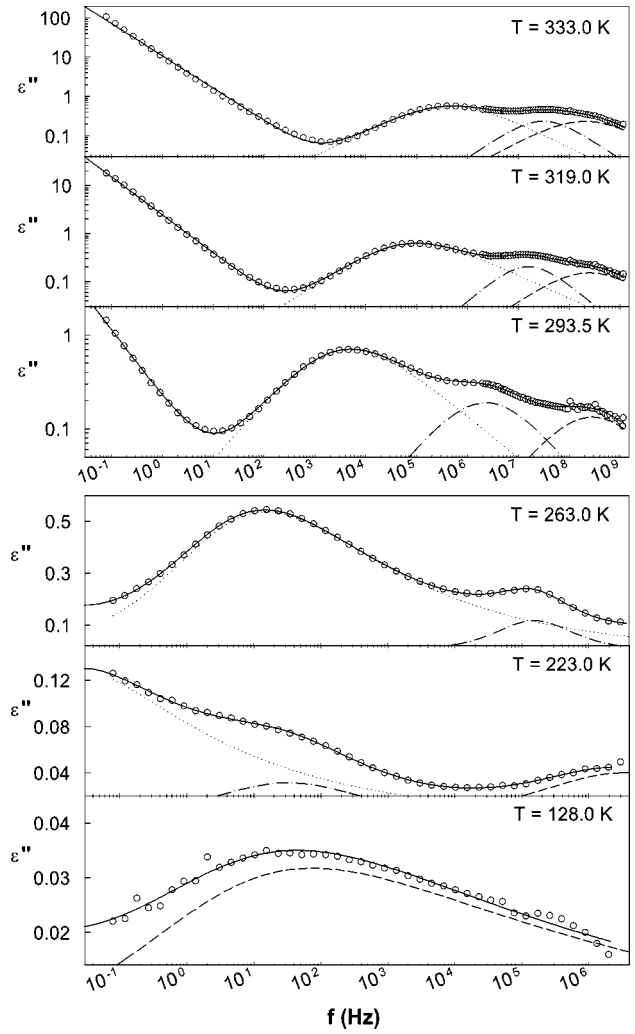

FIG. 5. The imaginary parts of the dielectric permittivity of 10CB embedded in porous Vycor glass at different temperatures. The symbols are data points and the solid lines show fitting according to Eq. (2). The broken lines represent deconvolution into elementary processes: the dashed lines represent the bulklike libration motion of molecules, the dash-dotted lines represent the bulklike process due to rotation of molecules around short axis, and the dotted lines represent the surface process.

aniline, nitrobenzene and dioxane molecules, with the hydroxyl groups on the surfaces of porous silica glasses prepared by the sol-gel process [51]. The strong surface interaction, however, was absent for weakly interacting liquids cyclohexane and *cis*-decalin. The slowest relaxation process, observed in our case, could be assigned as a surface process because of two reasons. First of all most of the molecules are close to the glass surfaces leading to a most prominent slow process. Secondly, the process is slower than all bulk relaxation processes observed in 10CB. The characteristic frequencies at liquid crystalline temperatures are also comparable to that of the surface process observed for 10CB with aerosils. The different processes have been deconvoluted into elementary contributions shown as broken lines in the figure. In fact, no visible phase transition was observed for 10CB in Vycor porous glass. Based on the studies of magnetic resonance and calorimetry similar continuous evolution of the orientational order at the nematic-to-isotropic transition in pores of Vycor glass were reported [52]. The typical quadrupolar splitting expected for a nematic phase was not found for 5CB in Vycor, whereas the absorption peak was found to be 20 times larger than in the isotropic phase. The measurements were, however, limited to a narrow temperature range. This result was also supported by a theoretical work on small droplets, where the *N-I* transition in 5CB was predicted to become continuous below a critical enclosing size [53]. On comparing the α parameters, which take into account the distribution of relaxation times, for different confinement we see that the value increases. This increase in the distribution of relaxation times with decreasing confinement can be attributed to "size effect." We also found that for 10CB in Vycor no crystallization could be observed. The sample could be supercooled at least down to 123 K, the lowest accessible temperature at present in our lab. In Fig. 5 the spectra have been chosen at representative temperatures that clearly show the shifting of the relaxation processes as we cool down the sample. On top of that all the three processes were found to be quite broad even at isotropic temperatures where α is around 0.35 for the fastest process, 0.2 for molecular rotation around short axis, and 0.3 for the surface process. All of these values increased gradually to values around 0.7 as we lowered the temperature to around 123 K. The surface process is asymmetric with β reducing from 1 at isotropic temperatures to 0.2 down at the lowest temperatures. The dielectric strength of this process increased as we lowered the temperature. The temperature dependence of the dielectric strength of the bulklike processes on the other hand decreased, although weakly, as we lowered the temperature. The fitting parameters obtained for the curves in Fig. 5 are given in Table I. In short, we observe a deep supercooling of the phase and broadening of the bulklike spectra in the very narrow Vycor channels in contrast to that observed for 10CB in other confinements—aerosils and anopore membranes.

V. TEMPERATURE DEPENDENCE OF RELAXATION TIMES

The temperature dependence of the relaxation times of the main bulk processes observed for 10CB are shown for parallel (rotation around short axis) and perpendicular (librational motion) orientations in Fig. 6. In the isotropic and smectic phases, the dielectric behavior is quite typical for an nCB. The logarithms of the relaxation times are linear with the inverse temperatures in the isotropic and smectic phases for both orientations of the director. The corresponding activation energies in the isotropic and smectic phases in parallel and perpendicular orientation were found to be 61.9 kJ/mol, 42.8 kJ/mol ($\mathbf{E} \| \mathbf{n}$), and 5.0 kJ/mol ($\mathbf{E} \perp \mathbf{n}$), respectively.

The temperature dependence of the relaxation times of the process due to the rotation around the short axis for 10CB embedded in untreated Anopore membranes are also shown in Fig. 6. The process is always faster in Anopore membranes. In the isotropic phase this may not be real as the different values of β, which are different in bulk and Anopore, can lead to differences in the fitted values. However in

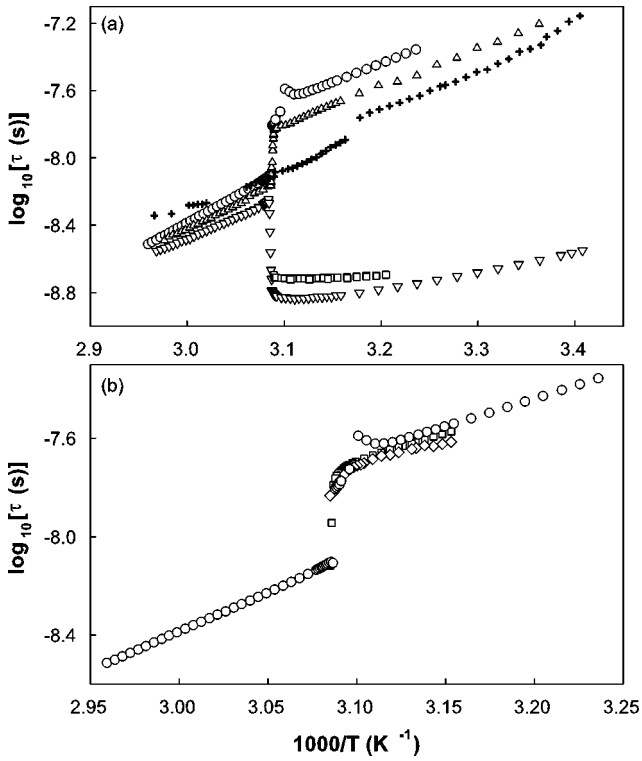

FIG. 6. Temperature dependence of the relaxation times $\tau(T)$ of the main bulklike processes for bulk and confined 10CB: (a) rotation of molecules around their short axes of bulk 10CB (○); librational motion of bulk 10CB (□); 10CB in untreated Anopores (△); 10CB in lecithin treated Anopores (▽); and bulklike rotation around short axis for 10CB in Vycor (+) shown in this figure limited to temperatures above the bulk crystallization temperature only. (b) Temperature dependence of the relaxation times $\tau(T)$ of the main bulklike processes for 10CB with 0.08 g cm^{-3} (□) and 0.31 g cm^{-3} (◇) aerosil samples. For comparison the relaxation times due to rotation of molecules around their short axes of bulk 10CB (○) have been included. Relaxations times for the aerosil samples and bulk values overlap due to very similar values.

the smectic phase the speeding up of the process could be real. This feature is also common in the nematic phase, as for example, for 5CB and 8CB in Anopores, where the process due to the rotation of molecules around their short axes is always faster in Anopores than in bulk [49]. The temperature dependence of the relaxation times of the process due to libration motion of the molecules for 10CB embedded in lecithin treated Anopore membranes are also shown in Fig. 6. The process has relaxation times close to bulk values obtained for the $\mathbf{E} \perp \mathbf{n}$ configuration. In the case of 10CB in lecithin treated Anopores there is only one process in the smectic phase, which has a activation energy of 19.4 kJ/mol. This value is slightly higher than the bulk value. In the isotropic phase the main relaxation has an activation energy of 48.5 kJ/mol that is quite similar to the value in case of untreated Anopore membranes as well as bulk 10CB.

The temperature dependence of the bulklike relaxation (rotation around the short axis) of 10CB with hydrophilic aerosils for both concentrations have been presented in the smectic phase in the same figure. In the Isotropic phase the process is out of the measured frequency range. It can be

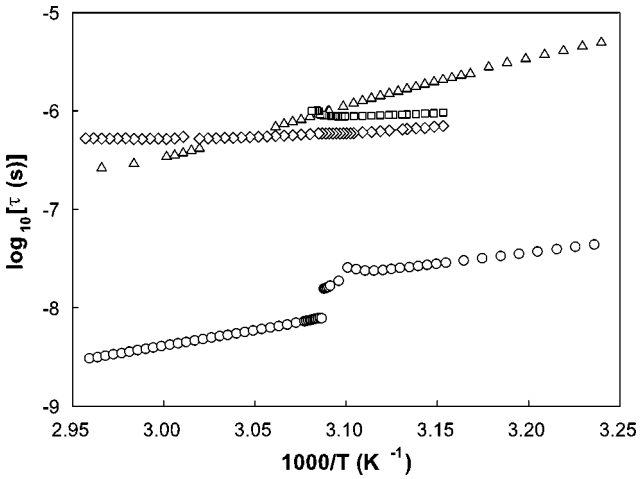

FIG. 7. Temperature dependence of the relaxation times $\tau(T)$ for the surface process of 10CB dispersed with hydrophilic aerosils: 0.08 g cm^{-3} (□); 0.31 g cm^{-3} (◇); and surface process for 10CB in Vycor (△) shown in this figure limited to temperatures above the bulk crystallization temperature only. For comparison the bulk relaxation times corresponding to the rotation around short axis has also been shown (○).

seen that the process has relaxation times very similar to the bulk process. The temperature dependence of the relaxation times of the surface processes observed for 10CB dispersed with aerosils, for both concentrations, has been shown separately in Fig. 7. The surface process seems to have a very weak temperature dependence that is merely affected by the phase transition, at least in the case of 10CB with 0.31 g cm^{-3} of aerosils. Overall, the temperature dependence of relaxation times of bulklike and surface processes presented till now have an activated type of dynamics in the isotropic and liquid crystalline phases. We see slight supercooling for both 10CB in Anopores and dispersed with hydrophilic aerosils, however, we do not see features of VFT-like temperature dependence maybe because the temperature range is too narrow.

The temperature dependence of the bulklike processes as well as the surface process of 10CB in Vycor is quite different from the other composites. First of all, in this sample the phase transition is replaced by a continuous variation of the relaxation process. For comparison see the relaxation times of the second process plotted along with the relaxation times of the process due to the rotation of molecules around their short axes obtained for 10CB in other confinements, shown in Fig. 6. In Figs. 8–10 we show the complete range of the relaxation times for the surface process, rotation of molecules around short axis, and librational motion of molecules respectively, for 10CB in Vycor. In the bulk phase the sample crystallized at 309 K. However in the pores of Vycor glass the sample is supercooled down to at least 123 K, which is roughly 185 K below bulk crystallization temperature. The Arrhenius plot of these relaxation times for a very wide temperature range shows features of glass-forming systems, i.e., the relaxation time does not have a linear dependence with respect to inverse temperature. The curvature in the Arrhenius plot indicates an increase in the rate of slowing down of

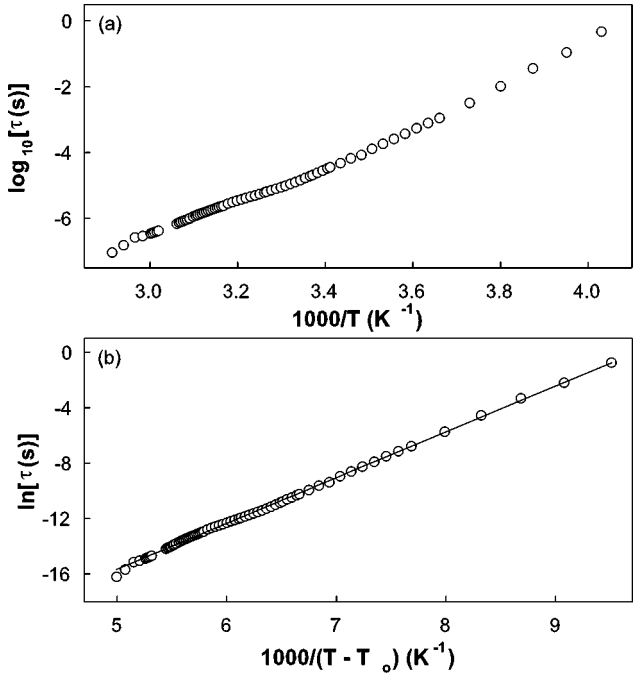

FIG. 8. (a) Temperature dependence of the relaxation times $\tau(T)$ for the surface process of 10CB in Vycor. (b) Dependence of the above relaxation as obtained by fitting to VFT temperature dependence. Symbols are data points and the solid line represents a linear fit. The value of T_0 in the figure is given in Table II.

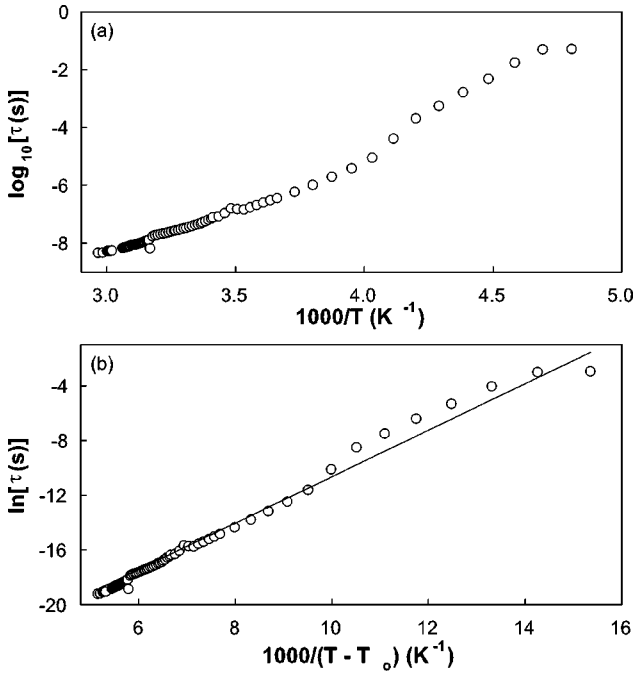

FIG. 9. (a) Temperature dependence of the relaxation times $\tau(T)$ for the bulklike process due to the rotation around short axis of 10CB in Vycor. (b) Dependence of the above relaxation as obtained by fitting to VFT temperature dependence. Symbols are data points and the solid line represents a linear fit. The value of T_0 in the figure is given in Table II.

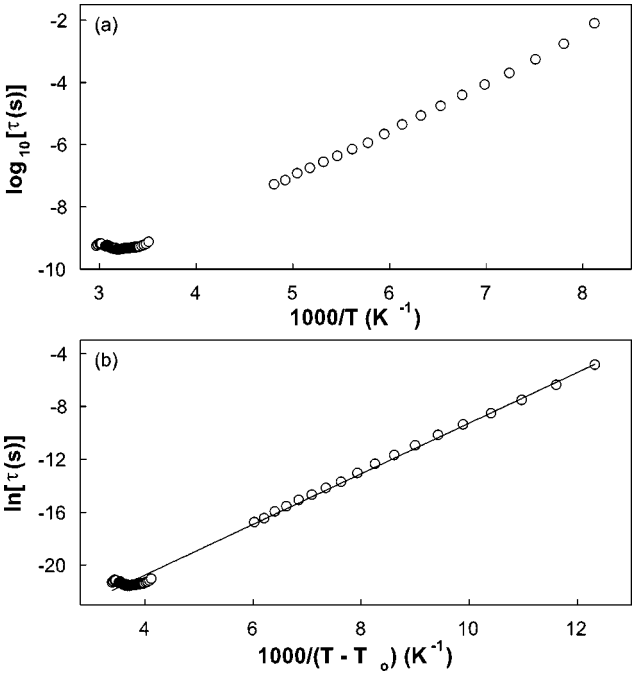

FIG. 10. (a) Temperature dependence of the relaxation times $\tau(T)$ for the bulklike librational motion of 10CB in Vycor. (b) Dependence of the above relaxation as obtained by fitting to VFT temperature dependence. Symbols are data points and the solid line represents a linear fit. The value of T_0 in the figure is given in Table II.

the relaxation times as we decrease the temperature. We were able to fit the relaxation times with the empirical Vogel-Fulcher-Tamman (VFT) law [54]:

$$\tau = \tau_0 \exp\left\{\frac{B}{T - T_0}\right\}, \tag{3}$$

typical for a glass forming liquid where, B is the fragility index, τ_0 is the limiting high temperature relaxation time, and T_0 is the Vogel temperature. The fitting parameters are given in Table II. It can be seen from Fig. 8 that the temperature dependence of relaxation times of the surface process shows features of a glass-forming system. Such behavior can happen, according to the Adam-Gibbs theory [55] based on the Kauzmann concept of configurational entropy, if there is some cooperativity between the relaxing molecules that increases as we reduce the temperature. It is possible that there is some cooperativity in the surface process that collectively propagates through the surface at low tempera-

TABLE II. Fitting parameters using Eq. (3) for relaxation times of 10CB in Vycor.

Process	$\ln\{\tau_0$ (s)$\}$	B (K)	T_0 (K)	T_g (K)
		10CB in Vycor		
Surface	−32.18	3305.0	143.0	232.8
Rotation	−27.60	1696.0	143.0	195.6
Libration	−28.39	1913.0	42.0	100.0

tures. The disorder in the surface layers and interfacial effects on 10CB embedded in Vycor may be the reason for the observed unusual behavior. Such a collective process is, generally, known to have glasslike slowing down due to increase in cooperativity upon approaching glass transition temperatures. In the study of a quasi-two-dimensional system of nCBs in aerosils where the LC molecules were mostly situated in the surface layers of the aerosils, a glasslike behavior was already observed [11]. The situation of 10CB molecules in the vicinity of the pore surface could be similar to that of the LC molecules near aerosil particles as reported in the above mentioned study. In Ref. [11] it was also found that a high fragility index D compared to the isotropic bulk state existed and it was concluded that the system was quasi-two-dimentional as higher D indicates weaker interaction. However, we also see features of a glass-former from the temperature dependence of the bulklike processes in Vycor porous glass. It should be stressed that these processes in bulk are non collective modes and thus should not be sensitive to the glass transition. In Fig. 9(a) which represents the temperature dependence of the process due to the rotation around the short axis in isotropic, smectic, and supercooled phases the curvature in the relaxation times is evident.

The temperature dependence of the libration mode could be followed down to the lowest temperature available (see Figs. 5 and 10). Hence in the case of the librational mode we have the widest possible range of temperatures. This bulklike process also has a VFT-like temperature dependence. However, we see the temperature dependence of this process is closer to a straight line in the Arrhenius plot of the relaxation times in comparison to the process due to the rotation of molecules around short axis. We can infer it also from the low value of T_0 compared to the other processes.

From the thermodynamics point of view Kauzmann showed that at T_k the configurational entropy will become zero if extrapolated smoothly from higher temperatures. He thus conjectured that a liquid-glass transition occurs at T_k where a change in the specific heat happens to avoid the violation of the third law of thermodynamics [56,57]. However, an absence or presence of a Kauzmann thermodynamic phase transition in glass formers is still a matter of debate [58,59]. Upon cooling liquids or liquid crystals below the crystallization temperature, the molecular motion slows down. For a sufficient fast rate of cooling the molecules do not reach the configurational state in the given time and crystallization is missed. At molecular relaxation times in the order of 100 s, the rate of change of volume (enthalpy) continuously reduces to solidlike values. The material thus reaches a glassy state [60].

Understanding quantitatively the extraordinary viscous slowing-down that accompanies supercooling and glass formation is still a major scientific challenge. In our case the experiments were more or less independent of the rate of cooling. In the case of Vycor porous glass the molecules residing in the pore segments, which have a diameter of 70 Å mostly contribute to the surface process. It is also evident from the dielectric spectra shown in Fig. 5 that most of the molecules are in the surface layers. However, it is known that the junctions of the pore segments have larger diameters in comparison to the segment [41], from where the bulklike processes may be arising. Thus the molecules contributing to the bulklike processes should be distributed in space separated by the pores segments. It is possible that the restriction of the LC phase into quasiseparated smaller domains, somehow, circumvents crystallization during cooling (even for moderate cooling rates). In the supercooled state the relaxation times and the viscosity increases dramatically where molecular rotations (and possibly low-energy vibrations) can still be observed. In this supercooled state the molecular rotations may also strongly couple to the translation dynamics, a characteristic of a glass former. However, the random pore surface, that destroy the long-range order of the phase in the pores may not be the true reason for circumventing crystallization, as such surface distortions are present in all the confined samples that we have presented. No such deep supercooling has either been observed for the widely studied decylcyanobiphenyl in confinements other than Vycor porous glass. From our above experiment we can say that we have added another parameter to the problem of glass formation where the diminutive size of confinement also leads to glassy behavior. The smaller the size of confinement the more the tendency of the material, that is of a nonglass former in bulk, to show features of a glass formation. However, we cannot rule out the possibility that these bulklike modes are no longer molecular modes under very small confinements. There could be some kind of strong coupling between molecules that causes glasslike behavior, which is weakly present for the other types of confinement. As it was observed from the fitting analysis the bulklike processes have a distribution of relaxation times, in contrast to that observed for the other confinements in this study. These spectra in the time domain representation would be transformed into stretch exponential function, which itself is indicative of a glass formation.

VI. CONCLUSION

The liquid crystal 10CB, with a direct isotropic–smectic-A transition, embedded in Anopore membranes and Vycor porous glass as well as dispersed with hydrophilic aerosils has been studied by dielectric spectroscopy. The temperature dependence of the static value of bulk 10CB in the smectic phase has a behavior that is different from a nematic phase observed in lower homologues of 10CB. The values of $\epsilon_{\|}$ were found to be lower than expected. This is most likely due to a smaller Kirkwood correlation factor in the smectic phase than in the nematic phase of the lower homologues. Additionally, the value of $\epsilon_{\|}$ decreases with decreasing temperature contrary to the dependence in a nematic phase. This effect could be due to a strong antiparallel correlation factor in 10CB as we lower the temperature. The temperature dependence of the static dielectric permittivity ϵ' of 10CB embedded in untreated and lecithin treated 2000 Å Anopore membranes as well as dispersed with hydrophilic aerosils were quite similar to the bulk dependence.

For bulk 10CB four dipolar relaxation processes are observed in the smectic phase—two for parallel alignment and two for perpendicular alignment. In the case of parallel alignment, one of the process has characteristic frequencies

around 5 MHz and is due to the rotation of molecules around their short axes and the other around 100 MHz is due to the molecular rotation in a cone around the director. In the case of perpendicular alignment the slow relaxation processes have similar characteristic frequencies as to the rotation of molecules around the short axis. The faster process in the perpendicular alignment could be due to librational motion of molecules.

In the case of 10CB in cylindrical pores, without any surface treatment, the dielectric spectra are basically due to the axial alignment of molecules where the smectic layers are oriented perpendicular to the pore axis. In the smectic phase, for the untreated Anopores, there exist two processes similar to the case of the bulk. In the case of lecithin treated Anopores the orientation of the LC molecules could have a radial orientation in the smectic phase. We thus measure the librational mode in this orientation.

In the case of 10CB dispersed with hydrophilic aerosils another process in addition to the bulklike processes is observed. The process has been attributed to be restricted rotation of molecules in surface layers. The dielectric spectra in the case of 10CB embedded in porous Vycor glass has at least three clear relaxation processes. The fastest process can be related to the bulklike libration motion of molecules, for molecules that are perpendicular to the probing field. The second intermediate process is also a bulklike process that is due to the rotation of molecules around the short axis. Both the bulklike processes are weak in strength in comparison to the slowest relaxation process. The slowest relaxation process is assigned as a surface process, similar in origin to the slow process observed for 10CB dispersed with aerosils. No phase transition was observed for 10CB in Vycor porous glass. In fact the sample could be supercooled down to 123 K, our lowest accessible temperature.

The temperature dependence of the relaxation times of the main bulk processes observed for 10CB for parallel (rotation around short axis) and perpendicular (librational motion) orientations in the smectic phase and in the isotropic phase are of Arrhenius type. In the case of 10CB embedded in untreated Anopore membranes the temperature dependence of the relaxation times of the process due to rotation around the short axis are similar to the bulk dependence. The temperature dependence of the relaxation times of the process due to the libration motion of the molecules for 10CB embedded in lecithin treated Anopore membranes is also similar but with a slightly higher activation energy. The temperature dependence of the bulklike relaxations of 10CB with hydrophilic aerosils, for both concentrations, are also very similar to the bulk processes. The additionally observed surface process, for 10CB dispersed with aerosil particles, seems to have a very weak temperature dependence that is merely affected by the phase transition. No significant differences in the properties of 10CB dispersed with aerosils were observed by dielectric spectroscopic measurements in comparison to *n*CBs dispersed with aerosils that have an intervening nematic phase.

The temperature dependence of the bulklike processes as well as the surface process of 10CB in Vycor is quite different from the other composites. The relaxation times of all these follow the empirical Vogel-Fulcher-Tamman (VFT) law typical for a glass forming systems.

We have shown that in the case of a non-glass-forming liquid crystal confined to different sizes of confinement the system tends to show a glassy behavior as we decrease the size of confinement. We found that the smaller the size of confinement, the more the tendency of the material that has a Arrhenius-like temperature dependence in bulk, to show features of glassy behavior.

ACKNOWLEDGMENTS

This work was supported by the National Fund for Scientific Research Flanders (Belgium) (FWO, Project No. G.0246.02) and by the Research Council of K. U. Leuven (project GOA-4, 2002).

[1] *Liquid Crystals in Complex Geometries Formed by Polymer and Porous Networks*, edited by G. P. Crawford and S. Zumer (Taylor & Francis, London, 1996).

[2] *Dynamics in Small Confining Systems V*, edited by J. Drake, J. Klafter, P. Levitz, R. Overney, and M. Urbakh, MRS Symposia Proceedings No. 651 (Materials Research Society, Pittsburgh, PA, 2001).

[3] F. M. Aliev, in *Access to Nanoporous Materials* (Plenum Press, New York, 1995), p. 335.

[4] S. Granick, Science **253**, 1374 (1991).

[5] T. Bellini, L. Radzihovsky, J. Toner, and N. J. Clark, Science **294**, 1074 (2001).

[6] A. Jakli, S. Borbely, and L. Rosta, Eur. Phys. J. B **10**, 509 (1999).

[7] L. Radzihovsky and J. Toner, Phys. Rev. Lett. **79**, 4214 (1997).

[8] X. l. Wu, W. Goldburg, M. Liu, and J. Xue, Phys. Rev. Lett. **69**, 470 (1992).

[9] G. S. Iannacchione, S. Park, C. W. Garland, R. J. Birgeneau, and R. L. Leheny, Phys. Rev. E **67**, 011709 (2003).

[10] S. Frunza, L. Frunza, H. Goering, H. Sturm, and A. Schoenhals, Europhys. Lett. **56**, 801 (2001).

[11] S. Frunza, L. Frunza, M. Tintaru, I. Enache, T. Beica, and A. Schoenhals, Liq. Cryst. **31**, 913 (2004).

[12] C. V. Lobo, S. K. Prasad, and D. S. S. Rao, Phys. Rev. E **69**, 051706 (2004).

[13] D. Kang, C. Rosenblatt, and F. M. Aliev, Phys. Rev. Lett. **79**, 4826 (1997).

[14] T. Jin, G. Crawford, R. Crawford, S. Zumer, and D. Finotello, Phys. Rev. Lett. **90**, 015504 (2003).

[15] A. Hourri, T. K. Bose, and J. Thoen, Phys. Rev. E **63**, 051702 (2001).

[16] G. Sinha, C. Glorieux, and J. Thoen, Phys. Rev. E **69**, 031707 (2004).

[17] Z. Kutnjak, S. Kralj, and S. Zumer, Phys. Rev. E **66**, 041702 (2002).

[18] Y. B. Melnichenko, J. Schuller, R. Richert, B. Ewen, and C. K. Loong, J. Chem. Phys. **103**, 2016 (1995).
[19] B. Jerome and J. Commandeur, Nature (London) **386**, 589 (1997).
[20] M. Ramazanoglu, P. Clegg, R. Birgeneau, C. Garland, M. Neubert, and J. Kim, Phys. Rev. E **69**, 061706 (2004).
[21] L. Radzihovsky and J. Toner, Phys. Rev. B **60**, 206 (1999).
[22] H. Stark, Phys. Rep. **351**, 387 (2001).
[23] L. D. Gelb, K. E. Gubbins, R. Radhakrishnan, and M. Sliwinska-Bartkowiak, Rep. Prog. Phys. **62**, 15731659 (1999).
[24] B. Jerome, Rep. Prog. Phys. **54**, 391 (1991).
[25] A. Huwe, F. Kremer, P. Behrens, and W. Schwieger, Phys. Rev. Lett. **82**, 2338 (1999).
[26] T. Bellini, N. J. Clark, and D. W. Schaefer, Phys. Rev. Lett. **74**, 2740 (1995).
[27] T. Bellini, M. Buscaglia, C. Chiccoli, F. Mantegazza, P. Pasini, and C. Zannoni, Phys. Rev. Lett. **88**, 245506 (2002).
[28] D. Feldman, Phys. Rev. Lett. **84**, 4886 (2000).
[29] G. Sinha and F. Aliev, Mol. Cryst. Liq. Cryst. Sci. Technol., Sect. A **358**, 155 (2001).
[30] H. Zeng, B. Zalar, G. S. Iannacchione, and D. Finotello, Phys. Rev. E **60**, 5607 (1999).
[31] *Broadband Dielectric Spectroscopy*, edited by F. Kremer and A. Schönhals (Springer-Verlag, Berlin, 2003).
[32] G. Sinha and F. Aliev, Phys. Rev. E **58**, 2001 (1998).
[33] F. Aliev, J. Non-Cryst. Solids **307**, 489 (2002).
[34] H. Zeller, Phys. Rev. Lett. **48**, 334 (1982).
[35] F. K. Ch. Cramer, Th. Cramer, and R. Stannarius, J. Chem. Phys. **106**, 3730 (1997).
[36] T. Bellini, N. Clark, and D. Link, J. Phys.: Condens. Matter **15**, S175 (2003).
[37] T. Moses, Phys. Rev. E **64**, 010702(R) (2001).
[38] M. Kreuzer, T. Tschudi, W. de Jeu, and R. Eidenschink, Appl. Phys. Lett. **62**, 1712 (1993).
[39] Degussa Corp., Silica Division, 65 Challenger Road, Ridge-Field Park, NJ 07660, USA. For technical data see the manufacturer's booklet AEROSIL.
[40] G. S. Iannacchione, C. W. Garland, J. T. Mang, and T. P. Rieker, Phys. Rev. E **58**, 5966 (1998).
[41] G. S. Iannacchione, G. Crawford, S. Qian, J. Doane, D. Finotello, and S. Zumer, Phys. Rev. E **53**, 2402 (1996).
[42] P. Levitz, G. Ehret, S. K. Sinha, and J. M. Drake, J. Chem. Phys. **95**, 6151 (1991).
[43] A. Oka, G. Sinha, C. Glorieux, and J. Thoen, Liq. Cryst. **31**, 31 (2004).
[44] G. Sinha, A. Oka, C. Glorieux, and J. Thoen, Liq. Cryst. **31**, 1123 (2004).
[45] S. Havriliak and S. Negami, Polymer **8**, 101 (1967).
[46] J. Thoen and T. K. Bose, in *Handbook of Low and High Dielectric Constant Materials and Their Applications* (Academic Press, San Diego, 1999), p. 501.
[47] C. J. F. Bottcher and P. Bordewijk, *Theory of Electric Polarization, Vol. 2* (Elsevier Science, Amsterdam, 1978).
[48] S. Urban, M. Massalska-Arodz, A. Wurflinger, and R. Dabrowski, Liq. Cryst. **30**, 313 (2004).
[49] S. Rozanski, R. Stannarius, H. Groothues, and F. Kremer, Liq. Cryst. **20**, 59 (1996).
[50] D. Wallacher, V. P. Soprunyuk, A. V. Kityk, and K. Knorr, Phys. Rev. B **66**, 014203 (2002).
[51] G. Liu, Y. Li, and J. Jonas, J. Chem. Phys. **95**, 6892 (1991).
[52] G. S. Iannacchione, G. Crawford, S. Zumer, J. Doane, and D. Finotello, Phys. Rev. Lett. **71**, 2595 (1993).
[53] S. Kralj, S. Zumer, and D. Allender, Phys. Rev. A **43**, 2943 (1991).
[54] *Disorder Effects on Relaxational Processes*, edited by R. Richert and A. Blumen (Springer-Verlag, Berlin, 1994).
[55] G. Adams and J. H. Gibbs, J. Chem. Phys. **43**, 139 (1965).
[56] R. Deegan and S. Nagel, Phys. Rev. B **52**, 5653 (1995).
[57] C. A. Angell, K. L. Ngai, G. B. McKenna, P. F. McMillan, and S. W. Martin, J. Appl. Phys. **88**, 3113 (2000).
[58] L. Santen and W. Krauth, Nature (London) **405**, 550 (2000).
[59] M. Jimenez-Ruiz, A. Criado, F. Bermejo, G. Cuello, F. Trouw, R. Fernandez-Perea, H. Lowen, C. Cabrillo, and H. Fischer, Phys. Rev. Lett. **83**, 2757 (1999).
[60] P. Debenedetti and F. Stillinger, Nature (London) **410**, 259 (2001).